Heritage Science

RESEARCH Open Access

Scientific analysis of two compound eye beads unearthed in Hejia Village, Zhouling

Jingyu Li[1], Feng Sun[1*], Yanglizheng Zhang[2], Wenhui Ha[1], Haihong Yan[1] and Congwen Zhai[1]

Abstract

The glass compound eye bead is the exquisite embodiment of the glassmaking technology of ancient craftsmen, and is an example of the cultural exchange between China and the West during the Warring States Period. This study takes two dots and mesh beads with seriously weathered surfaces excavated from Hejia village, Zhouling as the research object. Micromorphology, X-ray fluorescence spectroscopy (XRF), microscopic laser Raman spectroscopy and X-ray photoelectron spectroscopy (XPS) were respectively used to determine the chemical elements, valence states and compositions of the glass matrix and its weathering products. In this study, the valence state analysis of group-d elements is used to reveal the electron transition mode and explain the colour formation reason of blue-black glass matrix. In terms of weathering products, in addition to the identification of common cerusite [$PbCO_3$] and barite [$BaSO_4$], the study also found the blue weathering product alforsite [$Ba_5(PO_4)_3Cl$] for the first time. The study also makes reasonable assumptions about the reasons for their appearance. The X-ray photoelectron spectroscopy (XPS) used in this study has positive significance for the study of the formation mechanism of glass colour. The scientific and technological analysis data of these two glass beads provide basic data for the related research of the lead-barium glass system produced in China, and also provide a certain scientific basis for the related protection research.

Keywords Dots and mesh beads, X-ray photoelectron spectroscopy, The colour of glass, Alforsite, Weathering mechanism

Introduction

Glass compound eye beads are a type of bead decorated with an eye pattern. It is often called dragonfly eye bead in China because it resembles the shape of a dragonfly's eye. In western countries it is called "compound glass eye bead". Glass compound eye beads first appeared in ancient Egypt in the 18th dynasty (around 1400 BC) as a decoration on coffins, mummies and other artefacts [1–3]. Because their appearance is associated with the "evil eye" consciousness, glass compound eye beads are also called "evil-eye beads" by anthropologists. The earliest appearance of glass compound eye beads in China can be traced back to the period between the end of Spring and Autumn and the beginning of the Warring States period (around 475 BC) [4]. The glass compound eye beads that appeared at this time were thought to have been imported from Central Asia, providing a physical example of ancient Chinese and foreign cultural exchange [5, 6]. After the Warring States period, Chinese-made glass compound eye beads were excavated in Hunan and Hubei regions [7]. Unlike the imported beads, which had a higher content of sodium and calcium, the Chinese-made beads had a higher content of lead and barium, and were very popular in Chu. Glass compound eye beads have been found in the late Warring States Period burials of civilians in Hunan and Hubei [8], and

*Correspondence:
Feng Sun
sunfeng@nwu.edu.cn
[1] China-Central Asia "Belt and Road" Joint Laboratory On Human and Environment Research, Key Laboratory of Cultural Heritage Research and Conservation, School of Cultural Heritage, Northwest University, Xi'an 710127, Shaanxi, People's Republic of China
[2] Shaanxi Academy of Archaeology, Xi'an 710054, China

were used for decoration in the following ways Coffin decorations; Baldric (head, chest, waist; worn alone or in combination; regardless of gender; tool inlays (inlaid with bronze mirrors, jade, lacquer, bone or bamboo pins [9].

Hejia village, Zhouling is located in the former site of Hejia Village, Zhouling, Weicheng District, Xianyang, Shaanxi Province, on the second-level platform on the north bank of the Weihe River. 10.4 kms east of the site of Xianyang City of Qin, 1.7 kms northwest is the Mausoleum of King Wu of Zhou. These tombs are believed to be among the civilian tombs of Xianyang City of Qin. A large number of lead-barium-silicate artefacts, including glass beads, have been unearthed from the site.

There are two glass eye beads in this study, as shown in Fig. 1. **Sample 1**: Archaeological number M709:3–1. The color of the bead is yellow. The bead is almost flat at both ends. Beaded, height 18.3 mm, maximum diameter 21.3 mm, aperture 7.5 mm. **Sample 2**: Archaeological number M961:7. The color of the bead is blue. The bead is almost flat at both ends. Beaded, height 18.7 mm, maximum diameter 21.3 mm, aperture 8.5 mm. The two samples have the same size and similar decoration. Their patterns are: The dotted mesh pattern fills in the gaps between the eye pieces and makes the eye pattern more symmetrical. The mesh separates the eyes on the surface of the beads to form several independent small units. Archaeologically, these two compound eye beads belong to the dots and mesh bead [9] or the H-shaped geometric line spacing eye bead [10].

Fig. 1 Compound eye beads unearthed in Hejia Village

This type of bead first appeared in the early Warring States period in the M14 tomb of Qiancheng, Huaihua, Hunan Province [11]. It was also found in Chenxi, Hunan Province and Wangshan, Hubei Province during this period. The object diagram of the dots & mesh bead, which is similar in shape to the small reticulated dragonfly eye glass beads unearthed in Hejia Village, Zhouling, is summarised in Fig. 2 [9, 10]. In the early Warring States period, this type of compound eye bead was very popular in Hunan and Hubei. In the Middle and Late Warring States Period, it began to appear in Sichuan, Shaanxi and Hebei, and was still popular in Guangdong in the Qin and Han dynasties. In addition, this type of compound eye bead has been excavated mainly in Hunan, Hubei, Sichuan and other areas strongly influenced by Ba & Chu culture. Therefore, this type of dots & mesh bead has a very close relationship with the Ba & Chu culture [12].

Research aim

In recent years, the scientific and technological research of glass eye beads mainly focuses on the discussion of the formation reason of the glass matrix [13, 14] and

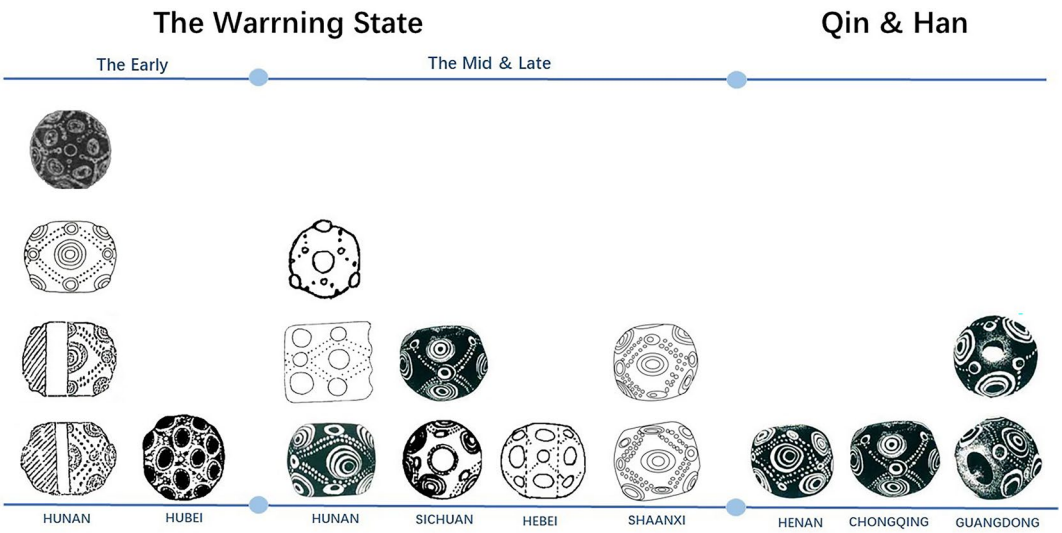

Fig. 2 Dots and mesh beads unearthed by China

the analysis and identification of weathering products [14–17]. The color formation mechanism is mostly based on the results of elemental analysis of the sample using XRF or LA-ICP-AES technology. Most of the weathering products were analyzed by Raman spectroscopy, and the weathering results of $PbCO_3$, $BaSO_4$, barium silicate, lead silicate and other common lead-barium silicate systems were concentrated.

In order to further explain the color formation mechanism from the electron transition mode of the colored group-d elements, in this study, X-ray photoelectron spectroscopy (XPS) was first used to analyze the valence state of color elements of glass beads. And the two similar glass beads showed obvious different weathering products of yellow and blue, which should be closely related to the burial environment. The weathering mechanism was further deduced by using micro-laser Raman spectroscopy to qualitatively analyze its composition.

Methods

OM analysis

The microscopic morphology of the glass beads was observed using a super depth of field 3D microscope (HIROXKH-7700 model from Japan). The observation aimed to study the state of preservation, colour and detailed information of these beads. The sample surface was observed at 100 × and 400 × magnifications, and the most suitable representative area was later selected for subsequent analysis.

X-ray fluorescence spectrometry

Bruker ARTAX400 mobile micro area X-ray fluorescence spectrometer. Test conditions were voltage 30 kV, current 900 μA, atmosphere helium and test time 300 s.

Raman spectroscopy

The physical phase structure of the samples was investigated using Raman spectroscopy. It was carried out using a Thermo Fisher DXR 2 Raman Spectroscopy equipped with a 633 nm laser at the laboratory of the College of Chemistry and Materials Science, Northwest University in Xian, China.

X-ray photoelectron spectroscopy

PHI5000VersaProbe III X-ray photoelectron spectrometer manufactured by ULVAC-PHI. The excitation source is Al Kα. The instrument is used for the detection of valence changes of Cu and Fe elements in matrix and of glass samples and for the discussion of the colour formation mode of glass.

Results

Micromorphology

A small part of the weathered layer is scraped off the surface of the samples and a small area of the sample substrate is obtained. The surface of the samples is observed by ultra deep field microscopy at 100-fold field and 400-fold field, respectively. The surface observation results of the two beads are shown in Fig. 3. A is the observation results of the bare surface of the beads at 100×, b is the observation results of the selected areas in the red box in Fig. a at 400×, and c is the observation result of the weathered products on the surface of the beads at 100×.

The figure shows that the surface of the two samples is heavily weathered. The substrate is dark blue. Large areas of the weathered layer on the surface are coarse and yellow. The weathered layer in the vicinity of the substrate in the sample is all of the shiny white substances or the accumulation of the milky yellow shiny substances. However, due to the presence of blue weathered layer in the weathering products on the surface of Sample 2, these weathering products are mixed with yellow crusts, making the surface of the sample appear as a large area of light blue to the naked eye.

Therefore, X-ray fluorescence spectral analysis is performed on the substrate and the weathered layer of the samples. The substrate, white weathered layer, yellow weathered layer and blue weathered layer are analysed by Raman spectroscopy.

Elemental composition

To ensure the scientific data, X-ray fluorescence spectrometry was carried out at three random points in the substrate and regolith of the two samples. The quantitative analysis results of the elemental composition by X-ray fluorescence spectra of the compound eye beads excavated in Hejia Village, Zhouling are shown in Table 1.

The BaO and PbO contents in the substrate are 7.7%–11.8% and 1.6%–6.7% respectively. Therefore, the two glass beads are probably lead-barium glass. The PbO content of Sample 2 is higher than that of sample 1 and the BaO content is lower than that of Sample 1, making the substrate of Sample 2 more transparent than that of sample 1. This can also be seen in the photograph of the substrate (Fig. 3) at 400 × magnification as observed by micromorphology.

The BaO content in the weathered layer of the samples ranged from 1.9% to 21.7%. The BaO content in regolith points 2 and 3 of Sample 1 is significantly higher than that in the substrate, but the BaO content in regolith points 1 and 2 of Sample 2 is significantly lower than that in the substrate. This means that the distribution of barium on

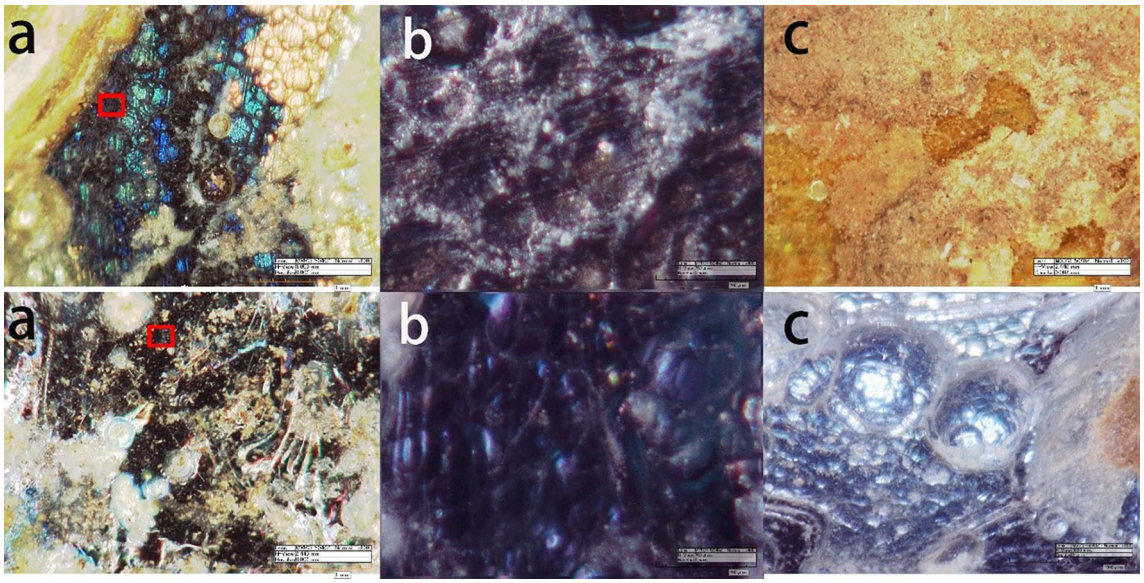

Fig. 3 Microscopic observation of samples. Sample 1 (above), Sample 2 (below)

Table 1 Chemical compositions of glass compound eye beads excavated from Hejia village of Zhoulin (wt%)

Sample	1						2					
Region	Matrix			Regolith			Matrix			Regolith		
Content	1	2	3	1	2	3	1	2	3	1	2	3
Na_2O	0.65	0.37	2.03	0.08	0.83	0.68	0.75	0.87	1.25	0.78	0.61	0.81
MgO	0.26	0.58	1.04	0.01	0.98	0.87	0.01	0.15	0.50	0.01	0.19	0.19
Al_2O_3	0.50	1.10	1.96	0.02	1.84	1.64	0.01	0.29	0.95	0.01	0.36	0.36
SiO_2	77.42	77.54	73.71	70.12	41.28	35.35	79.07	78.64	79.97	71.62	71.81	75.92
P_2O_5	0	0.06	0.22	0.33	2.27	2.26	0.60	0.58	0.01	0.64	0.88	0.05
K_2O	2.05	2.32	1.74	1.70	0.51	0.35	1.12	0.89	1.64	0.66	0.96	1.55
CaO	1.33	1.54	1.71	3.33	2.22	2.14	0.98	0.84	1.12	0.88	1.06	1.18
TiO_2	0	0.02	0.11	0.37	0.44	0.66	0	0	0	0.03	0.03	0.04
V_2O_5	0.09	0.10	0.11	0.10	0.15	0.26	0.05	0.06	0.04	0.06	0.05	0.07
MnO	0	0.12	0.64	2.38	2.06	1.87	0	0	0	0.36	0.35	0.31
Fe_2O_3	0.74	1.25	1.80	2.79	1.07	1.10	0.72	0.43	0.74	0.57	0.71	0.99
CuO	0.64	0.39	0.40	0.27	0.29	0.21	0.89	0.84	0.79	0.64	0.60	0.75
ZnO	0.03	0.01	0.01	0.01	0.02	0.01	0.02	0.02	0.02	0.01	0.01	0.02
SrO	0.13	0.46	0.66	0.56	0.67	1.06	0.08	0.08	0.10	0.12	0.11	0.12
SnO_2	0.09	0.10	0.06	0.16	0.54	0.45	0.05	0.16	0.24	0.77	0.72	0.41
Sb_2O_3	0.03	0.07	0.04	0.08	0.14	0.24	0.05	0.03	0.03	0	0	0.01
BaO	6.74	6.19	5.91	5.90	13.24	21.72	3.72	5.47	1.65	3.28	1.99	3.08
PbO	9.29	7.80	7.86	11.80	31.44	29.13	11.88	10.64	10.93	19.57	19.57	14.14

the weathered layer of the samples is not uniform, and some barium-rich regions have formed. In the study on the corrosion characteristics of lead-barium glass in the Qin dynasty, it was also found that the distribution of barium element in the weathered layer of sample MB-10 was not uniform, and some barium-rich regions were formed, and this barium-rich region was detected by Raman spectroscopy as a mixed state of lead carbonate and barium sulfate [18]. Therefore, it is believed that the uneven distribution of the barium element on the surface

was caused by the good water solubility of the barium salt. That is, the barium in the regolith is lost to the burial environment with water during the burial process, resulting in the uneven distribution of barium on the weathered layer.

The PbO content in the weathered layer is higher than that in the substrate, ranging from 11.8% to 31.4%. According to the result of the lead content on the surface of the substrate, these two glass beads are both low-lead glass at this time. The precipitation of lead is closely related to the temperature, humidity and pH of the buried environment. In the acidic environment of high temperature and high humidity, glass is easily eroded in the burial environment. The Pb content of the weathered layer of the samples is up to about 20% higher than that of the substrate, which also means that the surface structure of the substrate of the samples has been destroyed by long-term erosion in the buried environment [19, 20]. Therefore, more attention should also be paid to the control of lead precipitation in the conservation of silicate cultural relics.

Physical phase structure

The results of the Raman spectrum analysis of the substrate of the two beads are summarised in Fig. 4. The Raman spectra of the matrices of the two beads showed an envelope around 500 cm^{-1} and 1000 cm^{-1}, respectively, which corresponds to the bending and stretching vibration of the Si–O bond in the glass [21], and there were no obvious characteristic peaks in other regions of the two beads. This indicates that the matrices of the two beads are glassy.

The Raman spectral analysis results of yellow, white and blue weathered layer of samples 1 and 2 are shown in Figs. 5, 6 7.

From the results of the Raman spectra, it can be seen that the yellow weathered layer in Samples 1 and 2 is cerusite [$PbCO_3$]. The white weathered layer shows a mixture of barium sulphate [$BaSO_4$] and cerusite [$PbCO_3$]. This may be related to the choice of points, as the white particles are surrounded by a large area of yellow weathered layer, so it is assumed that the main component of the white weathering products is barium sulphate. The large area of blue weathered layer covered by Sample 2 is alforsite [$Ba_5(PO_4)_3Cl$].

Discussion

Glass matrix colour formation mechanism

The presence of d-metals in glass materials is the main cause of their colouration. The effect of the ligand field (LF) generated by the metal neighbours induces energy splitting of the d-orbitals. The colour results from the light excitation of the unpaired d-electrons, and the energy of the transition is determined by the properties of the d-metal, such as charge, polarisation, size and electronic configuration, and by the nature of the ligands and their arrangement around the metal, i.e. the coordination geometry. Common examples are aqua-blue caused by octahedral Fe^{2+}, green caused by Fe^{2+} & Fe^{3+}, and blue-turquoise caused by octahedral Cu^{2+}. It is clear that these colours are different from the dark blue glass matrix in this study. The contents of CuO and Fe_2O_3 range from 0.4% to 0.8% and 0.4% to 1.8% respectively, which are considered to be the result of the interaction

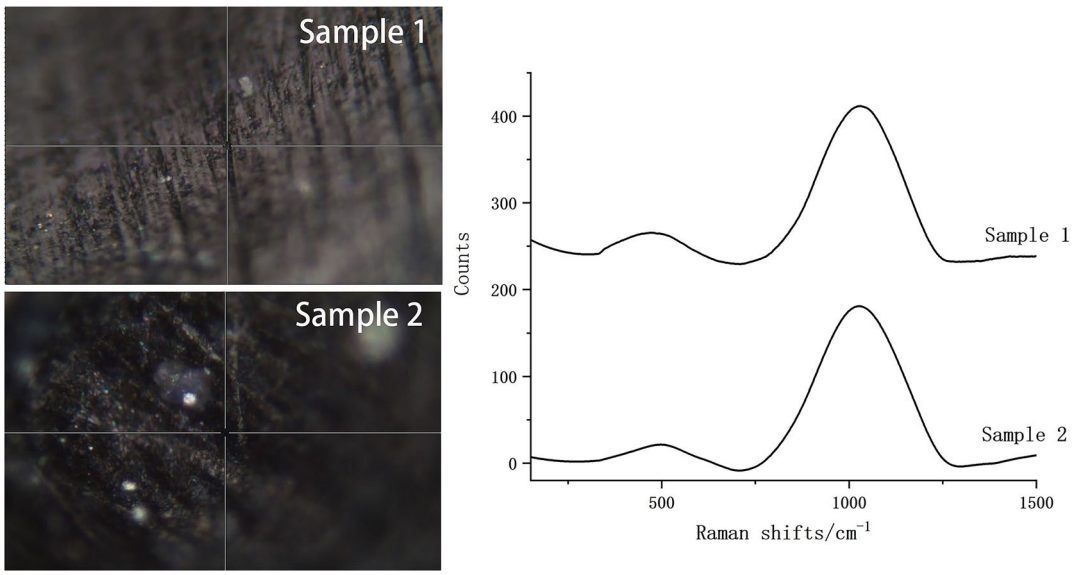

Fig. 4 Raman spectrum of body of Samples

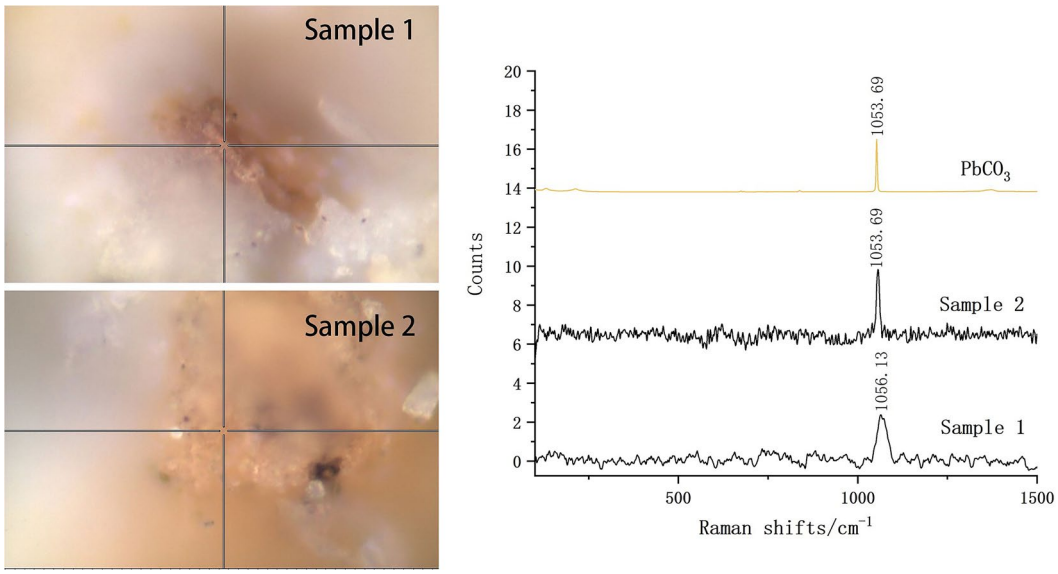

Fig. 5 Raman spectrum of yellow weathered layer of Sample 1 and 2

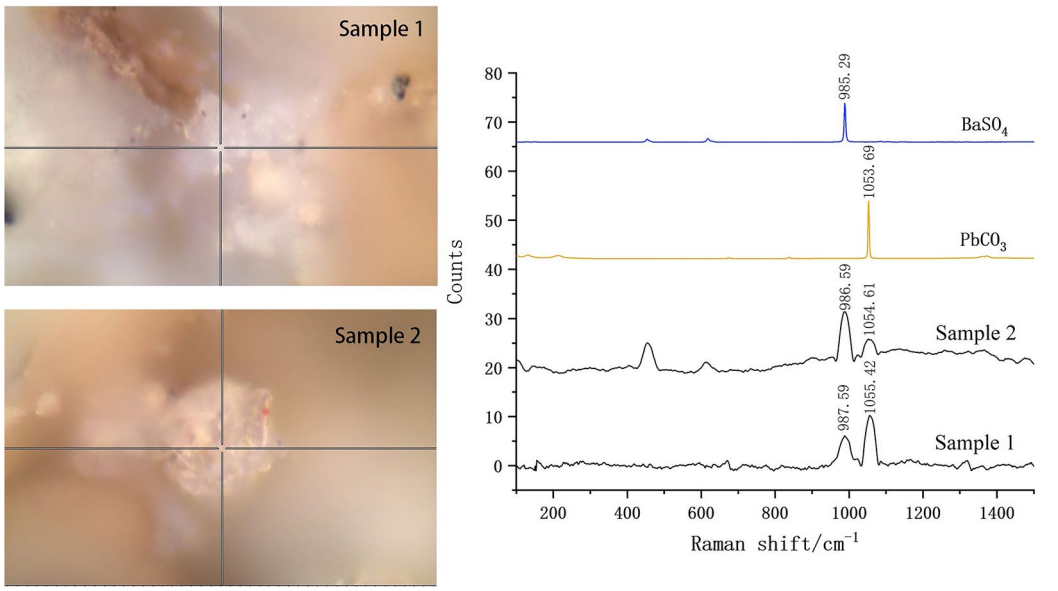

Fig. 6 Raman spectrum of white weathered layer of Sample 1 and 2

of Fe and Cu elements. The valence state of the element is very important to explain the mechanism of colour, so it is analysed by X-ray photoelectron spectroscopy.

Taking the XPS analysis of the matrix of Sample 1 as an example, the 2p spectral lines of Fe and Cu elements were fitted by peak splitting. It can be seen from the calculation that the quantitive ratio of Fe^{2+} to Fe^{3+} is 18.1%/81.9%, and the quantitive ratio of Cu^{+} to Cu^{2+} is 41.7%/58.3%. There are complex distributions of different valence states of different group-d elements in the glass matrix. Significantly, the intense coloration of some glasses cannot be explained only in terms of LF but also considering the contribution of the charge transfer transition, CT, so called because leading to a redistribution of electron density in metal complexes. This dark color is most likely due to intervalence charge transfer (IVCT) between different valence states of the same element [22].

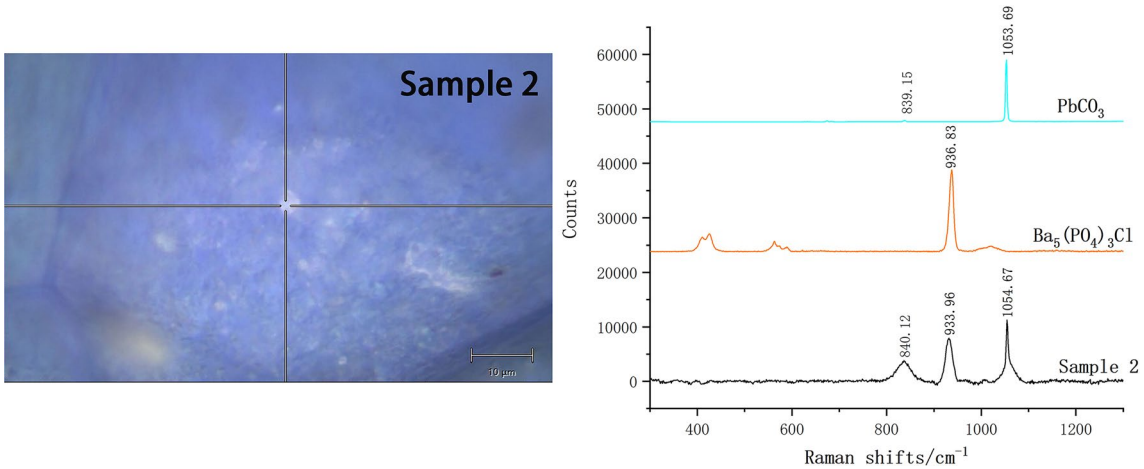

Fig. 7 Raman spectrum of blue weathered layer of Sample 2

Weathering mechanism

Cerussite [$PbCO_3$] itself is a warm-toned white in color, and is usually thought to yellow gradually during oxidation to a pale yellow in impurity. The formation process of cerussite is roughly as follows: lead oxide on the surface of glass beads combines with water in the buried environment to transform into a white, amorphous colloidal precipitate or solid, $PbO\text{-}xH_2O$ [23]; and then reacts progressively with carbonates in the environment on the surface of the glass beads, slowly transforming into the more stable white or yellow $PbCO_3$.

The formation of barium sulphate [$BaSO_4$] should be: due to better water solubility, Ba element in the lead-barium glass substrate collected on the surface of the glass, with the loss of water molecules [18]. And the barium element that has not been lost is captured by SO_4^{2-} in the soil on the glass surface and reacts to form barium sulphate.

Blue alforsite [$Ba_5(PO_4)_3Cl$] should be the first discovery of glass weathering products. $Ba_5(PO_4)_3Cl$ and $Ca_5(PO_4)_3Cl$ are isomorphism. That is, Ba takes the place of Ca, so the macro also appears as a sapphire lustrous blue. Alforsite belongs to the apatite group and is extremely rare in nature. The generation of this product should be inseparable from its special soil burial environment. The source of P element is most likely the proximity of Sample 2 to the corpse, which is the phosphate generated by the decay of the corpse. The Cl element should come from the water-salt transportation brought by the groundwater. Under the action of microorganisms such as fungi, a series of biochemical reactions occurred, and finally the apatite-like compounds, which are extremely rare in nature, were obtained. The presence of a large number of fungal microorganisms in the vicinity of the corpse can produce significant damage to the glass surface [23–26]. Moreover, the metabolites of the microorganisms accelerate the destruction of the glass network structure and the formation of corrosion pits [14]. After the decay of the corpse the phosphate in it enters the sample corrosion cracks, combines with the Ba ions lost from glass weathering, and then further reacts with the Cl ions brought about by the water-salt transport in the soil environment, ultimately generating alforsite [$Ba_5(PO_4)_3Cl$], a special weathering product.

In addition, although the two samples are similar in size and shape, the surface weathered layer on the surface are different due to the different burial environments. From the weathering products, it can be seen that the burial environment of sample 1 is stable, but the moisture in the environment leads to a large loss of Ba in its substrate, resulting in the reaction of the lead element with poor water solubility on the surface with carbonate, resulting in the accumulation of a large area of $PbCO_3$ on the surface. As the burial site of Sample 2 is close to the corpse, there is more phosphoric acid and fungi around it, so that the rare blue weathering product alforsite is produced in the right environment (Fig. 8).

Conclusions

In this study, micromorphology, X-ray fluorescence spectroscopy (XRF), microscopic laser Raman spectroscopy and X-ray photoelectron spectroscopy (XPS) are used for the chemical elements, valence states and compositions of the matrices and the weathering products of two dots and mesh glass beads, respectively. The reason for the colour formation of the dark blue glass matrix is elucidated. With regard to the identification of weathering products, alforsite [$Ba_5(PO_4)_3Cl$] is identified for the first time and

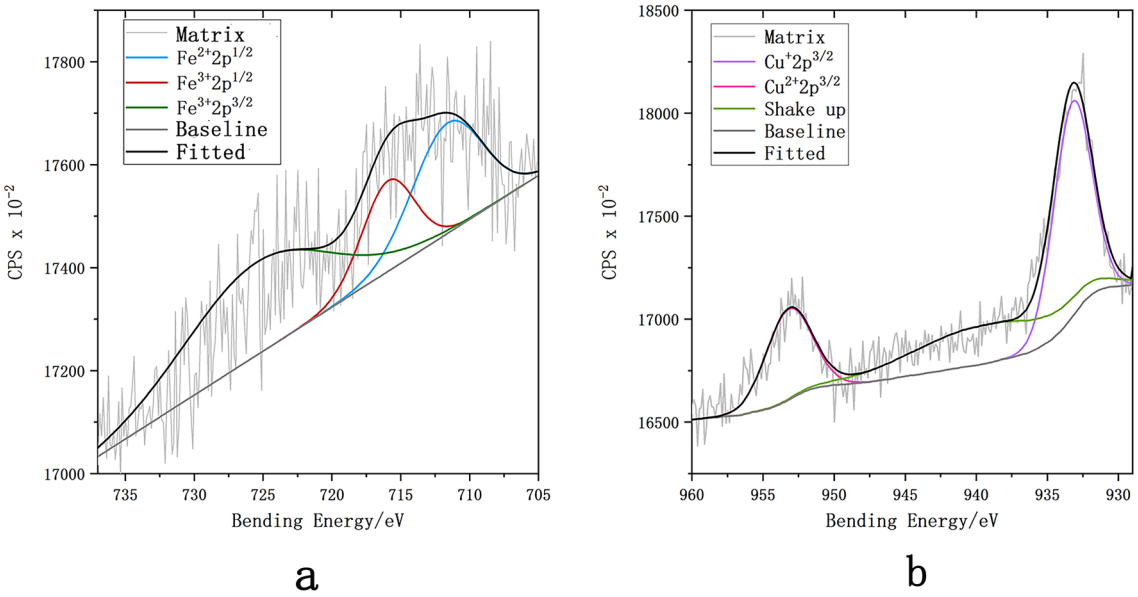

Fig. 8 XPS of dark blue matrix of Sample 1

the cause of its formation is reasonably speculated. The X-ray photoelectron spectroscopy used in this study has positive significance for the study of the formation mechanism of glass colour. The scientific and technological analysis data of these two glass beads provide basic data for the related research of the lead-barium glass system produced in China, and also provide a certain scientific basis for the related protection research.

Acknowledgements
The authors would like to thank the staff working at Hejia Village, Zhouling. They all gave us access to their facilities and waited patiently for us to finish our observations, photographs and samples.

Author contributions
All authors contributed to the conception and design of the study. Material preparation, data collection, and analysis were performed by JL, FS, and WH. YZ and FS provided the samples. The first draft of the manuscript was written by JL, and all authors read and revised the previous versions of the manuscript. All authors reviewed and approved the final manuscript.

Funding
This research was supported by the National Natural Science Foundation of China (Grant No. 22101226), 111 project (D18004).

Availability of data and materials
All data generated or analyzed during this study are included in this published article.

Declarations

Ethics approval and consent to participate
Not applicable.

Consent to participate
Not applicable.

Consent for publication
Not applicable.

Competing interests
The authors declare no competing interests.

Received: 27 October 2023 Accepted: 13 April 2024
Published online: 22 April 2024

References

1. Purowski T. Archaeometry. 2020;62(3):563–76. https://doi.org/10.1111/arcm.12543.
2. Tite MS, Maniatis Y, Kavoussanaki D, Panagiotaki M, Shortland AJ, Kirk SF. Colour in Minoan faience. J Archaeol Sci. 2009;36(2):370–8. https://doi.org/10.1016/j.jas.2008.09.031.
3. Yan HH, Sun F, Zhang YY. Scientific and technical analysis of lead-barium glaze dragonfly eye beads from the Late Warring States period in China. Herit Sci. 2023;11(1):186. https://doi.org/10.1186/s40494-023-01032-0.
4. Gan FX, Cheng HS, Hu YQ, Ma B, Gu DH. Study on the most early glass eye-beads in China unearthed from Xu Jialing Tomb in Xichuan of Henan Province, China. Sci China Ser E Technol Sci. 2009;52(4):922–7. https://doi.org/10.1007/s11431-008-0341-0.
5. Wu SY, Zhong JY, Ye H, Kang XS. Identification of ancient glass categories based on distance discriminant analysis. Herit Sci. 2023;11(1): 160.
6. Schibille N, Lankton JW, Gratuze B. Compositions of early Islamic glass along the Iranian Silk Road. Geochemistry. 2022;82(4): 125903. https://doi.org/10.1016/j.chemer.2022.125903.
7. Li JM, Tang BC. A preliminary study of glass compound eye beads in Zhongshan State of Warring States. Identif Apprec Cultural Relics. 2022;223(4):86–9.
8. Gao ZX. The characteristics of Warring States glassware unearthed in Hunan Province. Art of China. 1995;122:54–63.
9. Guan SM. Early China glass. Hongkong, China: The Chinese University in Hongkong Press; 2001.
10. Zhao DY. Studies on compound eye beads unearthed in China. Acta Archaeologica Sinica. 2012;02:181–7.

11. Xiang KW, Yang ZP, Shen SC. Brief report on excavation of Warring States Tombs in Qiancheng. Qianyang County J Hunan Archaeol. 1989;10:61–73.
12. Qin Y, Wang YH, Chen X, Li HM, Xu YY, Li XL. The research of burning ancient Chinese lead-barium glass by using mineral raw materials. J Cult Herit. 2016;21:796–801. https://doi.org/10.1016/j.culher.2016.04.003.
13. Li M, Wang J, Wang JL, Ma QL, Zhang ZG. Synthesis and Raman study on needlelike silicates in Ancient Chinese Pb-Ba glass in Qin and Han dynasties. J Raman Spectrosc. 2014;45(8):672–6. https://doi.org/10.1002/jrs.4534.
14. Zhang KX, Wang J, Yu WD, Zhao J, Yue XZ, Luo HJ. Corrosion mechanisms for lead-barium glass from the Warring States period. Herit Sci. 2023;11(1):79. https://doi.org/10.1186/s40494-023-00930-7.
15. Wang D, Wen R, Henderson J, Hu XJ, Li WY. The chemical composition and manufacturing technology of glass beads excavated from the Hetian Bizili site, Xinjiang. Herit Sci. 2020;8(1): 127. Doi: https://doi.org/10.1186/s40494-020-00469-x.
16. Yatsuk O, Gorghinian A, Fiocco G, Davit P, Francone S, Serges A, Koch L, Re A, Giudice AL, Ferretti M, Malagodi M, Iaia C, Gulmini M. Ring-eye blue beads in Iron Age central Italy-Preliminary discussion of technology and possible trade connections. J Archaeol Sci Rep. 2023;47: 103763. https://doi.org/10.1016/j.jasrep.2022.103763.
17. Giachet MT, Gratuze B, Ozainne S, Mayor A, Huysecom E. A phoenician glass eye bead from 7th–5th c cal BCE Nin-Bèrè 3, Mali: Compositional characterisation by LA-ICP-MS. J Archaeol Sci Rep. 2019;24: 748–758. Doi: https://doi.org/10.1016/j.jasrep.2019.02.032.
18. Wang YZ, Wang J, Ma QL, Sun WG. Scientific research on the corrosion of two Qin Dynasty lead-barium glass samples. Sci Conserv Archaeol. 2023;35(1):47–57. https://doi.org/10.16334/j.cnki.cn31-1652/k.20210602156.(inChinese).
19. Thickett D, Ling D. Investigation of weeping glass deterioration under controlled relative humidity conditions. Stud Conserv. 2022;67(6):366–72. https://doi.org/10.1080/00393630.2021.1892429.
20. Palomar T, Chabas A, Bastidas DM, Fuente DDL, Verney-Carron A. Effect of Marine aerosols on the alteration of silicate glasses. J Non-Cryst Solids. 2017;471:328–37. https://doi.org/10.1016/j.jnoncrysol.2017.06.013.
21. Krzątała A, Krüger B, Galuskina I, Vapnik Y, Galuskin E. Walstromite, $BaCa_2(Si_3O_9)$, from Rankinite Paralava within Gehlenite Hornfels of the Hatrurim Basin, Negev Desert, Israel. Minerals. 2020;10(5):407. https://doi.org/10.3390/min10050407.
22. Cartechini L, Miliani C, Nodari L, Rosi F, Tomasin P. The chemistry of making color in art. J Cult Herit. 2021;50:188–210. https://doi.org/10.1016/j.culher.2021.05.002.
23. Fan XP, Fu WB, Zeng Y, Zhao XW. Study of the corrosion of a Western Han bronze Fang unearthed at Dongtianpu Cemetery of Zhongxian County, Chongqing. Sci Conserv Archaeol. 2020;32(2): 57–63. https://doi.org/10.16334/j.cnki.cn31-1652/k.2020.02.007.
24. Rodrigues A, Gutierrez-Patricio S, Miller AZ, Saiz-Jimenez C, Wiley R, Nunes D, Vilarigues M, Macedo MF. Fungal biodeterioration of stained-glass windows. Int Biodeterior Biodegrad. 2014;90:152–60. https://doi.org/10.1016/j.ibiod.2014.03.007.
25. Shirakawa MA, John VM, Mocelin A, Zilles R, Toma SH, Araki K, Toma HE, Thomaz AC, Gaylarde CC. Effect of silver nanoparticle and TiO_2 coatings on biofilm formation on four types of modern glass. Int Biodeterior Biodegrad. 2016;108:175–80. https://doi.org/10.1016/j.ibiod.2015.12.025.
26. Pinto AMC, Palomar T, Alves LC, Silva SHMD, Monteiro RC, Macedo MF, Vilarigues MG. Fungal biodeterioration of stained-glass windows in monuments from Belém do Pará (Brazil). Int Biodeterior Biodegrad. 2019;138:106–13. https://doi.org/10.1016/j.ibiod.2019.01.008.

Publisher's Note